SNO-STR-90-124

Los Alamos

Los Alamos National Laboratory
Los Alamos, New Mexico 87545

memorandum

TO: Peter Doe, P-3, MS D449

DATE: September 7, 1990

FROM: T. Butler

MAIL STOP/TELEPHONE: J576/7-6578

SYMBOL: MEE-13:90-570

SUBJECT: CALCULATED BUCKLING LOADS FOR THE SNO VESSEL

Attached is a short report summarizing buckling calculations that I have performed for the SNO vessel. Several conclusions based on those calculations and other experience with buckling of thin-walled vessels follow.

1. Numerical calculations of buckling of a perfect sphere loaded with uniform pressure match the classical theory.

2. The calculated buckling load (uniform pressure) of the SNO vessel is about 84% of that for the perfect sphere and the buckling is localized near the discontinuities.

3. Buckling for the SNO vessel under hydrostatic load occurs at about the same pressure as it does for the uniform load except it is even more localized and occurs near the chimney.

4. The localization of buckling near the chimney/sphere interface implies that considerable attention should be paid to details in this area.

5. The support cable configuration does not affect the buckling load for hydrostatic loading.

6. ASME Code Case N284 recommends a capacity reduction value of 0.15 for this vessel geometry. Perhaps this should be used for uniform pressure, but would be overly conservative for the actual loading case. I would recommend a reduction factor of 0.20, which would result in increasing the thickness of the upper spherical wall to 1.56 inch.

7. A thicker wall in the chimney near its interface with the sphere would affect the buckling load because of the buckling location.

8. The lower spherical portion of the vessel could be much thinner than the upper portion (based only on buckling considerations).

9. Lateral loads at the chimney/sphere interface could significantly lower the pressure load that causes buckling.

10. The one case considered with built-in imperfections lowered the buckling load to 62% of the calculated value for "perfect" SNO geometry and 52% of the perfect sphere geometry with uniform loading.

TAB:cja

Cy: C. Anderson, MEE-13, MS J576
S. Girrens, MEE-13, MS J576
MEE-13 Files

BUCKLING CALCULATIONS FOR SNO SPHERE

by

Tom Butler
MEE-13

I. Theoretical Buckling Pressure

The theoretical buckling pressure for a perfect sphere is given below. The eigenvalue, λ, is the theoretical buckling pressure divided by the applied pressure, 1.9 psi in this case.

$$E := 180000. \quad psi$$

$$\mu := 0.35$$

$$t := 1.4 \quad in.$$

$$R := 237.7 \quad in.$$

$$p := 2 \cdot E \cdot \frac{\left[\frac{t}{R}\right]^2}{\sqrt{3 \cdot \left[1. - \mu^2\right]}}$$

$$p = 7.697 \quad psi$$

$$\lambda := \frac{p}{1.9} \qquad \lambda = 4.051$$

II. Finite Element Predictions with Two-Dimensional, Axisymmetric Model

The ABAQUS finite element code was used to predict buckling for the two-dimensional, axisymmetric case. The first case considered was a perfect sphere with a uniform pressure of 1.9 psi. Figure 1 shows the results for this case. the eigenvalue is 4.10, which is essentially equal to the theoretical eigenvalue given above. The next case considered was a perfect sphere with a hydrostatic pressure varying from 0.0 psi at the base to 1.9 psi the top. The predicted eigenvalue for this case is 4.16, which is again very close the the theoretical value. For the third case (Fig. 2) the chimney section was added to the sphere and the pressure varied from 0.0 to 1.9 psi. The eigenvalue for this case is 4.48, which is considerably above the theoretical value. There are two reasons for the difference. One is the stiffness effect of the chimney and the other is the fact that pressure is not being applied normal to the sphere where the chimney is located.

III. Finite Element Predictions with Three-Dimensional Model

The ABAQUS code was used for the three-dimensional calculations. Only portion of the chimney was included to reduce the model size. The lower portion of the sphere was modelled with a coarse mesh since buckling was not expected there for the hydrostatic load case. All of the structure was represented with the S8R5 shell finite elements in the ABAQUS code. Only one quarter of the structure was modelled and symmetry boundary conditions were used on the cut planes. The support cables were included by adding vertical restraints at the cable locations. The model had 2521 node points with six degrees of freedom per node.

The first case considered was a uniform pressure load of 1.9 psi (Fig. 3). The predicted eigenvalue was 3.40, somewhat lower that for the axisymmetric case described above. A lower value would be expected because we are no longer dealing with a geometrically perfect sphere and buckling mode shapes that are not axisymmetric are allowed. Next, the effects of an imperfect mesh were considered. The maximum radial "error" in the shell was approximately 1% of the radius. This error occurred periodically as can be seen from the static pressure displacement field shown in Fig. 4. The result of this imperfect mesh was to lower the eigenvalue to 2.12, which is 62% of the value for the perfect mesh and 52% of the theoretical eigenvalue for the perfect sphere. The final case considered was the actual hydrostatic load case where the pressure varied from 0.0 psi at the bottom of the structure to 1.9 psi at the top of the spherical portion of the structure. Here, the eigenvalue was predicted to be 3.29, which is slightly lower than the value for evenly distributed pressure.

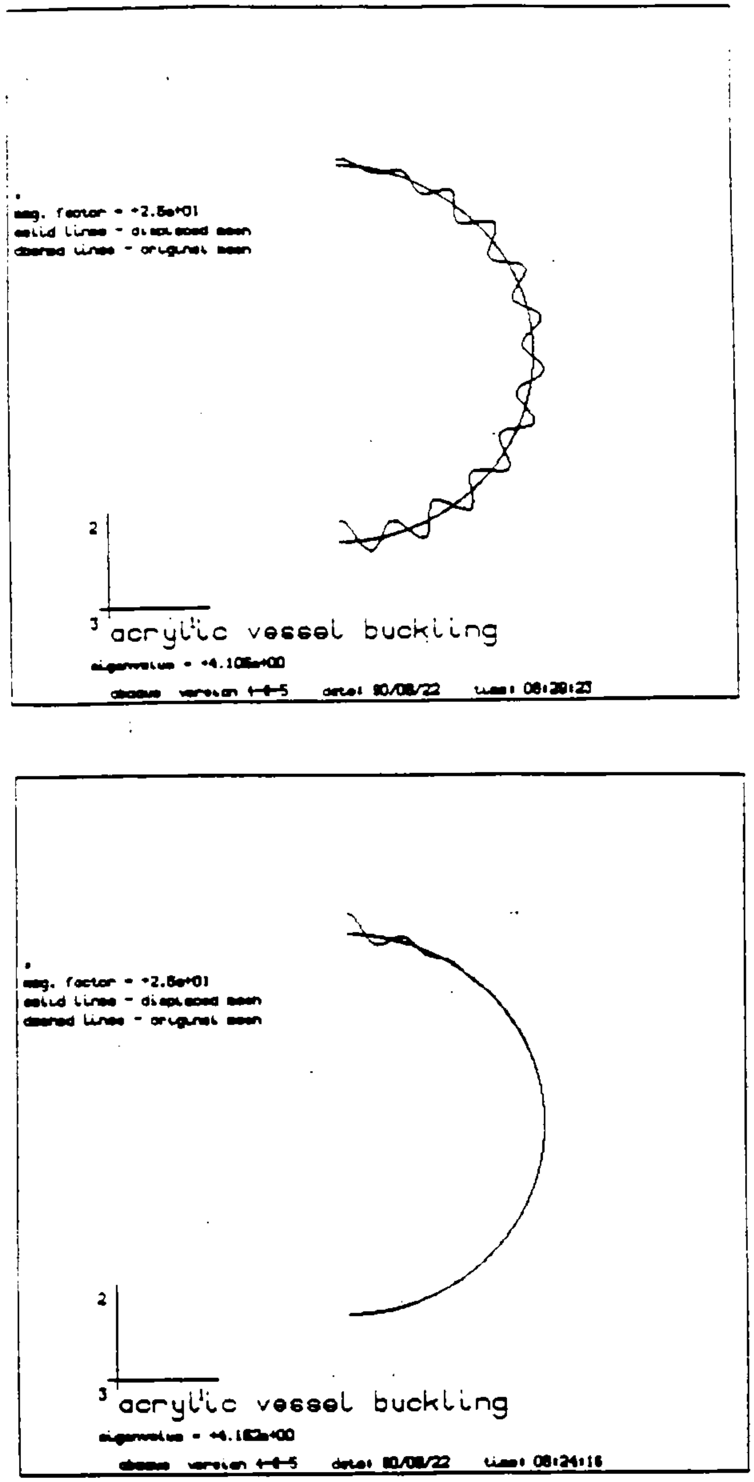

Fig. 1. Buckling mode shape and eigenvalue for axisymmetric sphere (top - uniform pressure, bottom - hydrostatic pressure 0.0 - 1.9 psi).

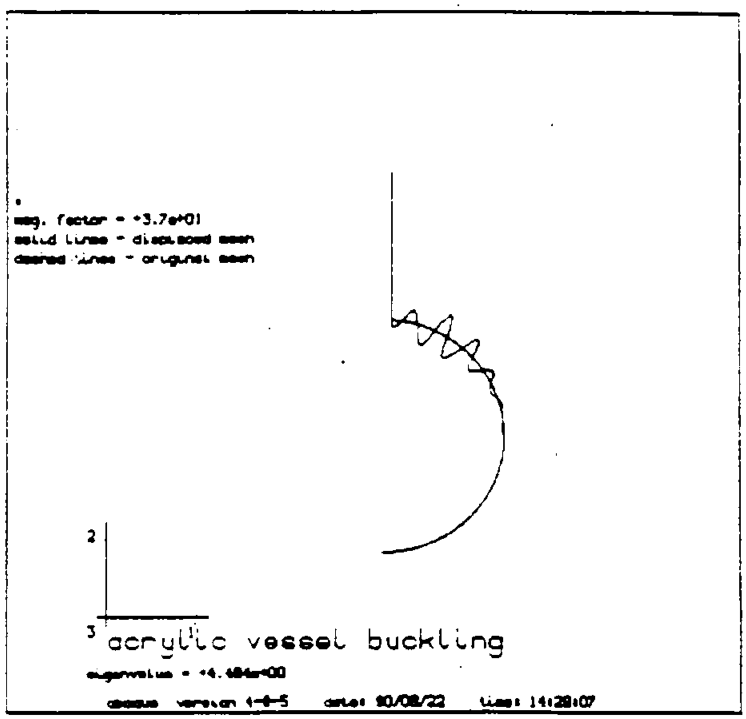

Fig. 2. Buckling mode shape and eigenvalue for axisymmetric representation of SNO vessel.

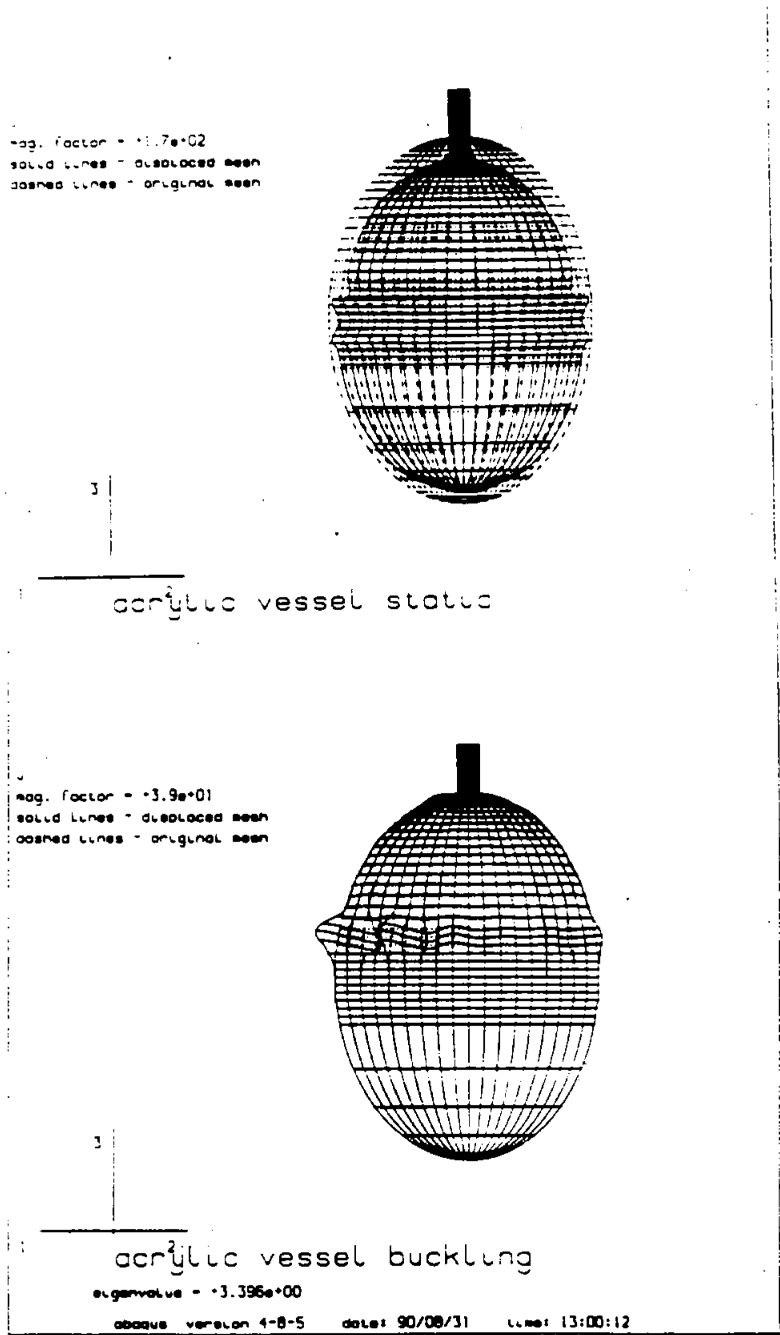

Fig. 3. Static displacement and buckling mode shape for SNO vessel with uniform 1.9 psi pressure load.

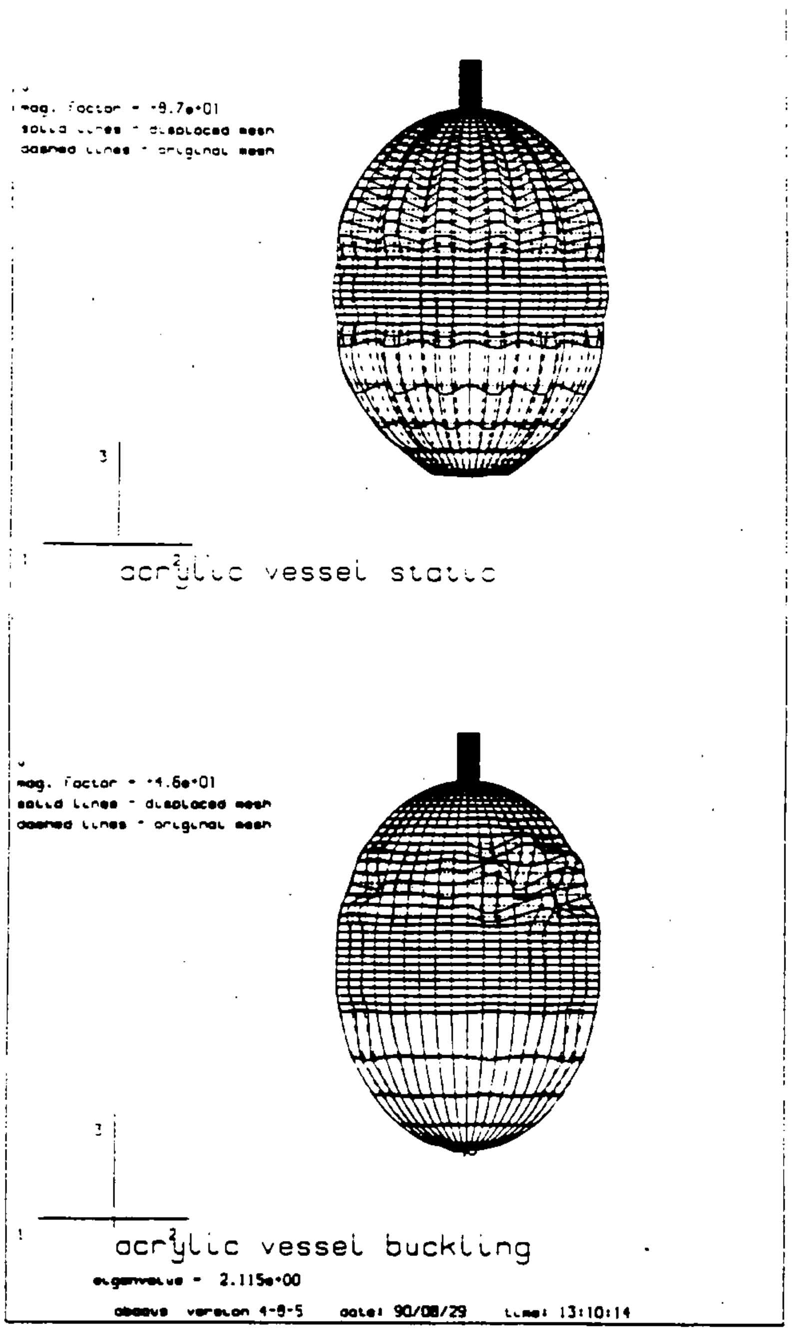

Fig. 4. Static displacement and buckling mode shape for SNO sphere with imperfect geometry and uniform pressure.

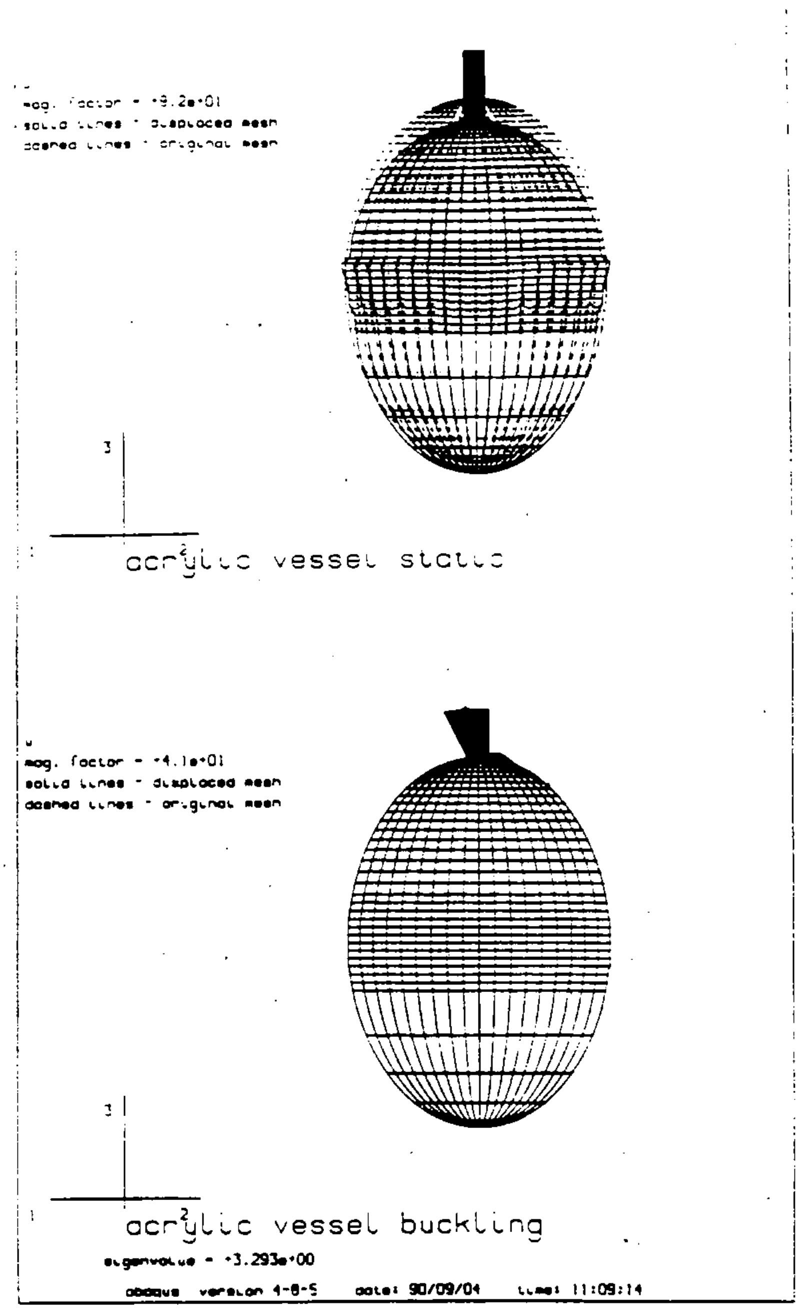

Fig. 5. Static displacement and buckling mode shape for SNO vessel with hydrostatic pressure load 0.0 to 1.9 psi.